Intelligent Multi-Sensor Measurements to Enhance Vehicle Navigation and Safety Systems

John W. Allen, Auburn University
Jordan H. Britt, Auburn University
Christopher J. Rose, Auburn University
David M. Bevly, Auburn University

BIOGRAPHY

John was born in Demopolis, AL and grew up in Birmingham, Alabama. In 2007, he obtained his bachelor's degree in Mechanical Engineering from Auburn University. Currently, John is working on his master's degree and works in the GPS and Vehicle Dynamics Lab. John's research interest includes multi-sensor fusion for vehicle navigation, and modern control theory for ground vehicles.

Jordan is currently a master's student and research assistant at Auburn University's GPS and Vehicle Dynamics Laboratory (GAVLAB). He received his B.S. degree in electrical engineering in 2008. His current research interests include sensor fusion and autonomous vehicle navigation and control.

Christopher Rose was born in Huntsville, Alabama. He is a member of the GPS and Vehicle Dynamics Lab at Auburn University. His current activities focus on video processing applications and sensor fusion in ground vehicles. He received his B.S. in Electrical Engineering at Auburn University in 2007.

David M. Bevly received his B.S. from Texas A&M University in 1995, M.S. from Massachusetts Institute of Technology in 1997, and Ph.D. from Stanford University in 2001 in mechanical engineering. He joined the faculty of the Department of Mechanical Engineering at Auburn University in 2001 as an assistant professor. Dr. Bevly's research interests include control systems, sensor fusion, GPS, state estimation, and parameter identification. His research focuses on vehicle dynamics as well as modeling and control of vehicle systems. Additionally, Dr. Bevly has developed algorithms for navigation and control of off-road vehicles and methods for identifying critical vehicle parameters using GPS and inertial sensors.

ABSTRACT

Nearly 50% of all the traffic fatalities are due to accidental lane departures. Therefore, there is great interest in advanced driver assistance systems to prevent unintended lane departures. The purpose of this paper is to present a method of lane positioning that involves combining a GPS/IMU navigation system with camera and Light Detection and Ranging (LiDAR) measurements. A discrete Kalman filter is implemented as the navigation filter used to combine all the measurements. The navigation coordinate frame is a coordinate frame attached to the road. The camera and LiDAR are assumed to give a measurement of the vehicle's current offset from the center of the current lane. This measurement directly corresponds to the y-axis of the navigation coordinate frame. The IMU used has 3 accelerometer axis and 3 gyros; however, only 2 accelerometers and 1 gyro were used for the navigation filter. Many vehicles come standard with a similar IMU set up for stability control.

Many issues become apparent when working with a shifting navigation frame. Measurements from the GPS must be mapped into the road coordinate frame. This involves a transformation from earth centered earth fixed (ECEF) coordinates to the road frame's coordinates. Also, the states of the navigation filter need to be updated when shifting to the next road coordinate frame. The largest implementation hurdle is obtaining a lane map. Current survey techniques are slow and require road closure. There are also issues with how long a road frame can be without adding error to the system. A road frame that is too long in a turn will cause error. The surveyed section of road used for the paper is split into road coordinate frames with an average length of around 10 m.

INTRODUCTION

In order to reduce the number of traffic fatalities that occur due to unintentional lane departures, many car

manufacturers are developing lane departure warning (LDW) systems that alert the driver before the vehicle departs the lane. Most of the LDW systems in production now are solely based off of camera measurements. Camera-based LDW systems are prone to failures due to road, weather, and lighting conditions. The purpose of this paper is to provide a method of sensor fusion that can be used to combine measurements from a camera, LiDAR, GPS receiver, and IMU to continuously measure lane position.

LiDAR stands for light detection and ranging. These devices are available on some vehicles equipped with active cruise control. The LiDAR scanner used for data collection is an IBEO ALASCA XT scanner. This scanner uses precise mirror movements to scan four horizontal scans in one scan cycle. The ALASCA XT is capable of reporting distance and reflectivity data, a measurement known as echo width. The reflectivity data reported will be used to distinguish lane markings from the road's surface using the principle that the lane markings should be more reflective than the road's surface at the same distance [6]. A more in-depth look at how the LiDAR is used to determine lane position can be found in [1].

Fig. 1. IBEO LiDAR Scanner with web camera

A GPS (global positioning system) receiver is useful for determining position on a global scale; however, a stand-alone GPS receiver is not precise enough to provide an accurate position of a vehicle within a particular lane on the road. Also, GPS can only provide position with respect to a global coordinate frame. For this project, position with respect to a lane is desired. Therefore, the only way GPS can be used for lane navigation is to construct a map of the lane. Even when compared to a map, stand alone GPS position is heavily biased and is not as accurate as vision methods for determining lane offset.

The camera used for data collection is a standard web camera. The camera is mounted directly below the LiDAR's focal point. The web camera takes a picture with every LiDAR scan. The image is thresholded to eliminate unwanted information. Edge detection and the Hough transform were employed to extract lane lines from the image. This image is then searched using polynomial bounds to find the position of the lanes and the vehicle's lateral position relative to the lanes. A more in-depth look at how the camera is used to determine lane position can be found in [8].

In order to provide a more robust measurement of lane position, the camera, LiDAR, and GPS measurements will be used to estimate the inertial measurement unit's (IMU) biases. A discrete Kalman filter is used to update lane position using the IMU, camera, LiDAR, and GPS. The IMU used to collect data is a microelectromechanical system (MEMS) automotive grade IMU. It has an update rate of 50 Hz. Therefore, the IMU can update lane position between vision and GPS updates. Also, the IMU is able to dead reckon the lane position for a small amount of time without any GPS, camera, or LiDAR measurements.

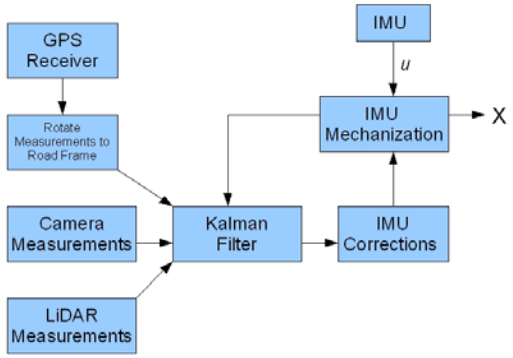

Fig. 2. Navigation Filter Architecture

In order to have an accurate baseline to compare results, RTK-corrected GPS position and velocity are recorded on all data runs. The GPS receiver used for data collection is the Novatel ProPak V3. The receiver is responsible for the RTK-corrected position and velocity solution. The Novatel's RTK-corrected position is also used in the track survey to obtain a lane map. All the GPS data used for the lane position algorithm development is non-differential (no corrections).

TRACK SURVEY

The proposed method of sensor fusion for lane position requires a detailed map of the lane in the which the vehicle is traveling. This is one limiting factor in implementation of the proposed method. Current GPS

receivers for personal vehicle navigation have a map database; however, in order to ensure accuracy, the map data base for this algorithm needs to be precise. GPS with RTK corrections can provide accuracy on the centimeter level; however, surveying using GPS can be time-consuming. Surveying lanes will also require the road to be free of traffic. Future development of lane positioning methods could be used to back out lane position relative to a known vehicle location [4]. Such systems would need to be based off differential GPS measurements and precise attitude determination.

Fig. 3. Top Down View of NCAT Track

All the data used for this paper was collected at the NCAT (National Center for Asphalt Technology) test track in Opelika, Alabama (Fig. 3). The track is a two lane 1.8 mile oval with flat straights and 8° of bank in the corners. The track is used to test wear on interstate asphalt. In order to accomplish this, the track is submitted to a fleet of tractor trailer trucks that drive on the track 16 hours a day, 5 days a week. The 1.8 miles of asphalt are divided into various segments with each segment containing asphalt from different locations in the Southeast and other locations in the USA. Some areas of the track have easily viewable lane markings. There are areas of the track where the middle (dashed) lane line is missing. The outside lane lines (solid) cover the majority of the track; however, there are a few spots where there is no outside lane line. One football field sized section of the back straight has no middle or outside lane lines. Also, there is one on-ramp, one off-ramp, and one service road intersection along the outside lane of the track. In these sections, the outside lane line is missing, and, the outside lane line runs off with the off-ramp.

In order to get a detailed map of the NCAT test track, the outside lane of the track was surveyed. The survey was conducted with two Novatel GPS receivers. Both of the receivers provide a narrow integer solution with corrections from an on-site base station. One GPS receiver was used to survey the middle lane line, and the other receiver was used to survey the outside lane line. The center lane line on the track is dashed at every 10 meters, roughly. The position of the center of each dash of the center lane line was surveyed. The outside lane was surveyed perpendicular to the road at every center lane line survey.

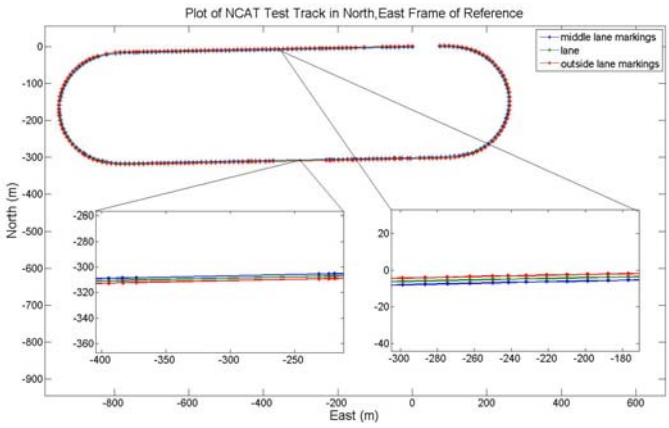

Fig. 4. Plot of NCAT Track Survey

To aid in surveying, two survey poles were used as GPS antenna mounts. The surveying poles provide a fixed antenna phase height off the ground. The poles are also equipped with a bubble to insure the pole is held upright. The GPS receivers used provides measurements of the GPS antenna location in earth centered earth fixed (ECEF) coordinates. The time average of the measurements was used to find the location. Time constraints limit the amount of time each spot can be surveyed. We averaged 10s worth of data at 10 Hz to determine the final position of the survey. Each recorded position was also corrected for the antenna height.

It is important to recognize that a GPS solution with RTK corrections is not an absolute measurement. There are considerable drifts from day to day. In order to get a more exact lane map, the position of the lanes needs to be observed over long periods of time. We have observed drifts in sub-meter magnitudes from day to day when working with our RTK set-up. The relative position obtained when surveying the track is very accurate. If, the track is surveyed on one day using the described survey method and then surveyed again on another day, the track maps will be the same but offset by some amount to the north and east. To overcome this, the track map can be offset by the north and east by a small amount by measuring drift at a known location close to the lane.

NAVIGATION FILTER

A Kalman Filter [5] is the core of the proposed lane tracking estimation algorithm. Since the inputs to the filter are discrete, a Discrete Kalman Filter is used. Many traditional navigation filters use the ECEF or tangential plane coordinates for navigation. The base navigation frame for this project is the tangential plane. The orientation of the plane is based off of the track map. The navigation frame is also called the road frame. The road frame is a coordinate frame that is attached to the road. The position and velocity states of the filter are expressed

in the road frame. The heading state (Ψ) is measured from the x-axis of the road frame.

$$X = \begin{bmatrix} x \\ y \\ \dot{x} \\ \dot{y} \\ b_{ax} \\ b_{ay} \\ \psi \\ b_{\psi} \end{bmatrix} \quad (1) \qquad u = \begin{bmatrix} \ddot{x} + b_{ax} \\ \ddot{y} + b_{ay} \\ \dot{\psi} + b_{\psi} \end{bmatrix} \quad (2)$$

The navigation filte is a 3 degree of freedom filter; therefore, the vehicle is assumed to neither pitch nor roll. Also, the vertical position and velocity of the vehicle is ignored. The first assumption does add error to the system; however, this error is small considering most roads are not pitched or banked at more than 10°.

NAVIGATION COORDINATE FRAME

A tangential coordinate frame is a frame of reference that is based off of a location given in longitude and latitude. For this work, the North East Down (NED) coordinate frame is defined as; x-axis pointing North, y-axis pointing East, and the z-axis is an axis that is pointed down. Heading can be measured as +/- 180° form the x-axis. The x- and y-axis of the coordinate frame lie in the plane tangent to the WGS84 ellipsoid. Geodetic longitude and latitude are used to describe the point on the ellipsoid at which the origin of the NED frame is located. Positions and velocities expressed in the ECEF frame can be mapped into the NED coordinate frame and vice versa. In order to move from the ECEF frame to the NED frame, the longitude and latitude of the center of the NED frame must be known. Also, the position of the center of the NED plane in ECEF coordinates must be known. Equation (3) shows the rotation matrix used to map positions and velocities in the ECEF frame to the NED frame.

$$R_{NED}^{ECEF} = \begin{bmatrix} -\sin(\phi)\cos(\lambda) & -\sin(\phi)\sin(\lambda) & \cos(\phi) \\ -\sin(\lambda) & \cos(\lambda) & 0 \\ -\cos(\phi)\cos(\lambda) & -\cos(\phi)\sin(\lambda) & -\sin(\phi) \end{bmatrix} \quad (3)$$

λ - Longitude of frame origin

ϕ - Latitude of frame origin

P_o - Position of frame origin in ECEF

$$P_{NED} = R_{NED}^{ECEF}(P_{ECEF} - P_o) \quad (4)$$

$$V_{NED} = R_{NED}^{ECEF}(V_{ECEF}) \quad (5)$$

Position measured in the ECEF coordinate frame can be mapped to the NED frame using (4) [3]. P_o is the position of the origin of the NED frame expressed in ECEF coordinates (P_o = [x y z]'). P_{ECEF} is the position of the point of interest in ECEF coordinates; P_{NED} is the position of the point of interest in NED coordinates. Velocities in ECEF coordinates (V_{ECEF}) can be directly rotated into the NED coordinate frame (V_{NED}) because the NED frame is not moving relative to the ECEF frame.

The base coordinate frame of the navigation filter is a modification of the NED frame. The data from the track survey is used to form a map of the surveyed lane. This map is based off of waypoints saved in ECEF coordinates. Each waypoint is located in the middle of the lane. The waypoints were calculated using the midpoint formula on each outside and middle lane line pair from the track survey. The navigation coordinate frame (road frame) is the same as the NED frame, except the x-axis points to the next waypoint the vehicle will pass. The origin of the frame is located at the last waypoint the vehicle passed.

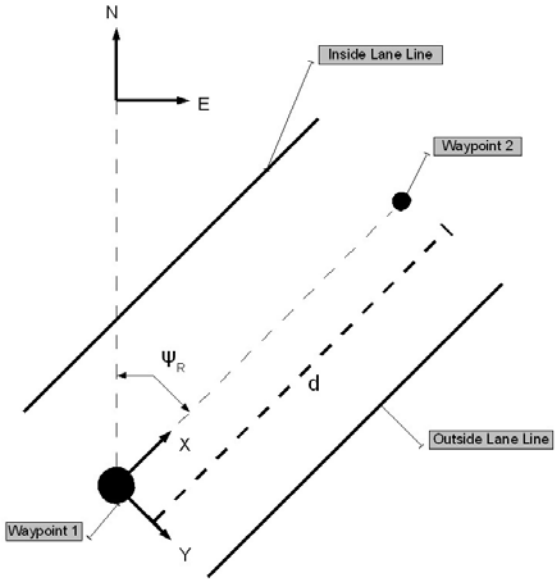

Fig. 5. Picture of Road Frame

Figure 5 shows a drawing of the navigation frame. Ψ_R is the road heading. The road heading is measured from the north-axis of the NED frame to the x-axis of the road frame. The length of the road frame is d. Once the vehicle passes the next waypoint, the road frame is shifted to a frame based on the waypoint the vehicle passed. Equation (6) is a matrix that maps coordinates in the NED frame to the road frame. It is based off of the angle Ψ_R.

$$R_{Road}^{NED} = \begin{bmatrix} \cos(\psi_R) & \sin(\psi_R) & 0 \\ -\sin(\psi_R) & \cos(\psi_R) & 0 \\ 0 & 0 & 1 \end{bmatrix} \quad (6)$$

Multiplying the rotation matrix from NED to road and the rotation matrix from ECEF to NED will result in a matrix that maps ECEF coordinates to road frame coordinates (7).

$$R_{Road}^{ECEF} = R_{Road}^{NED} * R_{NED}^{ECEF}$$

(7)

$$P_{Road} = R_{Road}^{ECEF}(P_{ECEF} - P_o) \tag{8}$$

$$V_{Road} = R_{Road}^{ECEF}(V_{ECEF}) \tag{9}$$

A total of 219 waypoints were used to construct the road frames; hence, there are 219 different road frames that make up the 1.8 mile track map. Each frame has 5 pieces of information associated with it: longitude of frame origin, latitude of frame origin, position of origin in ECEF coordinates, frame heading, and frame length. All this information is needed to map measurements from ECEF coordinates. These values are also needed to determine how and when to update road frames. If each road frame's coordinates are expressed in floating point format, all the information needed for 1 million miles (280 million road frames) can be stored in less than 8 gigabytes of digital storage.

IMU MECHANIZATION

The measurements from the IMU can be used to propagate the filters states between GPS, camera, and LiDAR measurements. Each state has a discrete time update function. The propagated state is a function of the previous state (x_{k-1}) and IMU measurement (u_{k-1}).

$$\hat{x}_k^- = f(\hat{x}_{k-1}^-, u_{k-1}) \tag{10}$$

$$f(\hat{x}_{k-1}^-, u_{k-1}) = \begin{bmatrix} x + (dt)\dot{x} + \frac{(dt)^2}{2}[(u_1 - b_{ax})\cos(\psi) - (u_2 - b_{ay})\sin(\psi)] \\ y + (dt)\dot{y} + \frac{(dt)^2}{2}[(u_1 - b_{ax})\sin(\psi) + (u_2 - b_{ay})\cos(\psi)] \\ \dot{x} + (dt)[(u_1 - b_{ax})\cos(\psi) - (u_2 - b_{ay})\sin(\psi)] \\ \dot{y} + (dt)[(u_1 - b_{ax})\sin(\psi) + (u_2 - b_{ay})\cos(\psi)] \\ b_{ax} \\ b_{ay} \\ \psi + (dt)[u_3 - b_\psi] \\ b_\psi \end{bmatrix} \tag{11}$$

Plugging the IMU outputs and current filter states into (11) will result in the filter states that have been propagated (dt) seconds into the future. The state covariance matrix (P) can be updated using (12) [9].

$$P_k^- = A_k P_{k-1} A_k^T + Q_{k-1} \tag{12}$$

A is a Jacobian matrix defined by

$$A_{[i,j]} = \frac{\partial f_{[i]}}{\partial x_{[j]}}(\hat{x}_{k-1}^-, u_{k-1}) \tag{13}$$

Q is the process noise covariance matrix. This matrix is assumed to be a constant diagonal matrix. The values of the diagonal elements of the process noise covariance matrix were hand-tuned to give desired performance.

MEASUREMENT UPDATE TYPES

A typical GPS/INS navigation system has only one type of measurement update. Adding a camera and LiDAR adds another type of measurement update. The camera and LiDAR are assumed to give measurements of the vehicle's current position in the lane, and an associated standard deviation with that measurement.

GPS

The GPS measurements are recorded in ECEF coordinates. The GPS receiver used to collect data also provides an estimate of the standard deviation of the receiver's position and velocity measurement. In order to update the filter, the GPS position must be mapped into the road frame using (8). The y measurement of position provided by the GPS is discarded. The vision methods provide a measurement of y to compensate for the GPS's y measurement. If no vision measurement is available, the navigation filter becomes unobservable; therefore, the GPS y measurement must be used to maintain observability. When no vision measurement is provided, the navigation filter will not provide lane level precision. The velocity measurement from the GPS can be mapped into the road frame using (9). The z component of the position and velocity in the road frame are also discarded. (14) and (15) show how to map the standard deviation of the position and velocity in ECEF coordinates to the road coordinate frame.

$$\sigma_{P,Road} = R_{Road}^{ECEF}(\sigma_{P,ECEF}) \tag{14}$$

$$\sigma_{V,Road} = R_{Road}^{ECEF}(\sigma_{V,ECEF}) \tag{15}$$

The Kalman gain is defined as [9]

$$K_k = P_k H_k^T (H_k P_k H_k^T + R_k) \tag{16}$$

R is the current measurement covariance matrix. The diagonal elements of this matrix are filled in using the standard deviations from (14) and (15) squared. H is the measurement matrix. If vision measurements are available, H is defined as

$$H = \begin{bmatrix} 1 & 0 & 0 & 0 & 0 & 0 & 0 & 0 \\ 0 & 0 & 1 & 0 & 0 & 0 & 0 & 0 \\ 0 & 0 & 0 & 1 & 0 & 0 & 0 & 0 \end{bmatrix} \tag{17}$$

If vision measurements are not available, H is defined as

$$H = \begin{bmatrix} 1 & 0 & 0 & 0 & 0 & 0 & 0 & 0 \\ 0 & 1 & 0 & 0 & 0 & 0 & 0 & 0 \\ 0 & 0 & 1 & 0 & 0 & 0 & 0 & 0 \\ 0 & 0 & 0 & 1 & 0 & 0 & 0 & 0 \end{bmatrix} \tag{18}$$

The state and covariance matrix can be updated using (19) and (20); where z_k is the measurement vector $\hat{z}_k$ is the predicted measurement vector using most current states.

$$\hat{x}_k = \hat{x}_k^- + K_k(z_k - \hat{z}_k) \quad (19)$$

$$P_k = (I - K_k H_k)P_k^- \quad (20)$$

LIDAR

The LiDAR will detect and track the lane markings through the use of bounding, discrimination, and by finding a best match solution to an expected value. Data taken from the LiDAR was at half-angle resolution. If multiple echo widths existed for a single half-angle measurement, then those echo widths were averaged together.

Because echo width data from the LiDAR can appear noisy at times due to precipitation or dead insects on the LiDAR screen, the on-road data can quickly become indistinguishable from erroneous or off-road data. To distinguish between these cases, the algorithm developed employees bounding. It establishes an area in front of the car that is approximately two lane widths wide. This width ensures that regardless of the vehicle's position in the lane or during a lane change, a lane marker can be found if one exists.

The lane markings are found by generating an ideal scan (Figure 6) and taking the minimum RMS error when compared to an actual scan. The ideal scan is generated by first averaging the echo widths located in a .6m wide area in front of the car. This averaged area represents the average reflectivity of the road's surface and is referred to as a baseline, which is the area between the spikes in Figure 6. The spikes in Figure 6 represent the actual lane markings, which are generated by simply multiplying the baseline by a factor of 1.75.

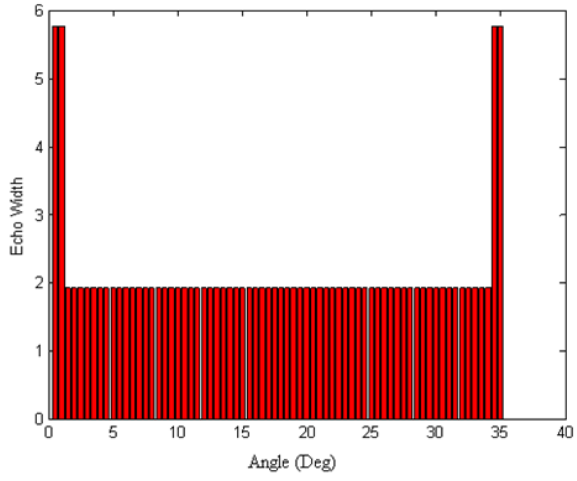

Fig. 6 Algorithm Generated Ideal Scan

Now that the basis for algorithm-generated ideal scan has been created, the RMS comparison can be performed. This is done by placing the leftmost side lobe at the leftmost scan boundary that was previously established and shifting it by half-angle increments until that side lobe has reached the center of the scan at zero degrees. With each shift of the left side lobe, the rightmost side lobe is placed at the center of the scan and stretched until the rightmost side lobe is equal to the rightmost scan boundary. The algorithm-generated ideal scan is stretched by simply adding in another baseline measurement between the side lobes.

To mitigate erroneous results with each shift, the distance between the leftmost side lobe and rightmost side lobe is checked to ensure that the width is greater than the minimum expected lane width and less than some maximum expected lane width, as set forth in [2]. The minimum RMS error generated from comparing the actual LiDAR scan to the algorithm-generated ideal scan is saved. The location of the innermost side lobes denote the lane angle corresponding to the lane marking. Using that information, the distance from the center of the vehicle to the lane marking can be computed. However, if lane markings reported by the RMS solution are not at least 1.4 times greater than the baseline, it is assumed a lane marking does not exist.

Distance results are then run through a low-pass filter to smooth out any jumps and a weighted average where the weights are based on the inverse of the variance for each layer's measurement. This simply gives preference to more consistent scans. Once these filtered distances have been computed, our offset from center is found.

CAMERA

The camera is also assumed to give the position of the vehicle within its current lane. A technique to eliminate erroneous lines has been employed which bounds the previously detected 2nd order polynomial with two other polynomials that are equidistant from the original polynomial. These bounding curves employ similar characteristics as the original curve; therefore, the valid lane marking should be detected within the bounded area given smooth transitions between each frame.

The effects of erroneous lines within this bounded area can be reduced by employing a Kalman filter on the coefficients of the 2nd order polynomial. The filter also allows for smooth transitions between curved and straight roads. The measurement of the position within the lane is carried out by determining the number of pixels from the center of the image and the estimated lane marking. This measurement value can then be converted to its real world

equivalent and used to estimate the position of the vehicle within the lane.

For vision updates, (16) is used to computed the Kalman gain. R is now a 1x1 matrix, which is equal to the variance of the current vision measurement. H is defined as

$$H = \begin{bmatrix} 0 & 1 & 0 & 0 & 0 & 0 & 0 & 0 \end{bmatrix} \tag{21}$$

Equation (19) is used to update the state, and (20) is used to update the covariance matrix.

NAVIGATION COORDINATE FRAME UPDATES

Since the navigation frame is based off of current position, the longitudinal position of the vehicle in the road coordinate frame must be checked after every state update. If the longitudinal position exceeds the length of the current road frame, then the vehicle has passed into the next road frame. The measurements of the states are expressed in the old road coordinate frame; therefore, the states must be mapped into the new road frame. If the vehicle has passed into the next road frame, the first step to update the states is to form a rotation matrix based off of the change in coordinate frame heading between the new and old coordinate frame (22). $\Psi_{R,i+1}$ is the heading of the new road coordinate frame and $\Psi_{R,i}$ is the heading of the old road coordinate frame.

$$R_{i+1}^{i} = \begin{bmatrix} \cos(\theta) & \sin(\theta) \\ -\sin(\theta) & \cos(\theta) \end{bmatrix} \tag{22}$$

$$\theta = \psi_{R\,i+1} - \psi_{R\,i}$$

The heading state can be updated by subtracting the change in coordinate frame heading from the current estimate of vehicle heading in the lane (23). Ψ_i is the estimated heading of the vehicle in the road coordinate frame. Ψ_{i+1} is the estimated heading of the vehicle in the new road coordinate frame.

$$\psi_{\,i+1} \;=\; \psi_{\,i} \;-\; \theta \tag{23}$$

The next step consists of updating the position state estimates. Equation (24) shows how to update the position states using the rotation matrix (22).

$$X_{i+1}^{pos} = R_{i+1}^{i}\left(X_{i}^{pos} - \begin{bmatrix} d_i \\ 0 \end{bmatrix}\right)$$

$$X_{i}^{pos} \text{ - Position in Road Frame (i)} \tag{24}$$

$$X_{i+1}^{pos} \text{ - Position in new Road Frame (i+1)}$$

The position state vector in (24) is a 2x1 vector ([x , y]'). d_i corresponds to the length of the previous road coordinate frame. Equation (25) shows how to map the velocity state vector into the new road coordinate frame.

$$X_{i+1}^{vel} = R_{i+1}^{i}\left(X_{i}^{vel}\right)$$

$$X_{i}^{vel} \text{ - Velocity in Road Frame (i)} \tag{25}$$

$$X_{i+1}^{vel} \text{ - Velocity in new Road Frame (i+1)}$$

After completing the above steps, the filter's state vector will be expressed in terms of the new road frame. This process must be performed every time the vehicle moves into a new road coordinate frame. Comparing the lateral position state (x) to d_i after every time and measurement update will ensure the navigation filter is operating in the appropriate road coordinate frame.

RTK-CORRECTED GPS POSITION AND VELCOITY BASELINE

A base-line is needed to compare the results of the navigation filter. The base-line used for this paper is GPS with RTK corrections. The RTK solution is provided by the GPS receiver. The receiver uses CMR corrections broadcasted from an on-site base station. The corrected position and velocity of the vehicle is saved in ECEF coordinates at 2Hz.

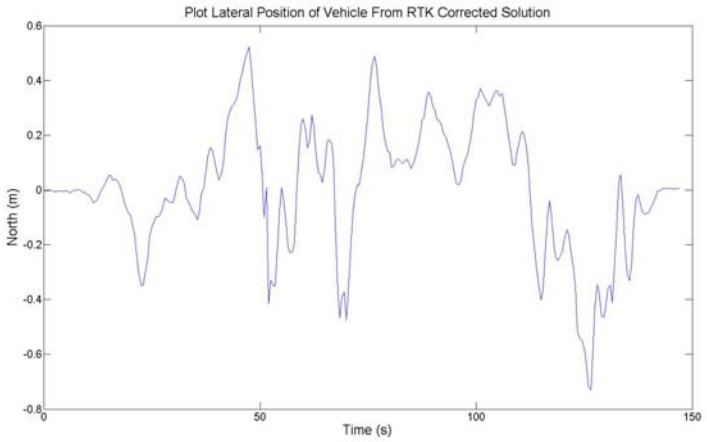

Fig. 7. Lateral Position of Vehicle Using RTK Solution

Figure 7 shows the lateral lane position of the vehicle for 147 seconds of data taken at the NCAT test track. Data from this run is used for all of the results. The vehicle starts on the first straightaway facing west and then travels around the track counter-clockwise. In addition, the vehicle accelerates from a stop to 50 mph and maintains this speed for the remainder of the lap.

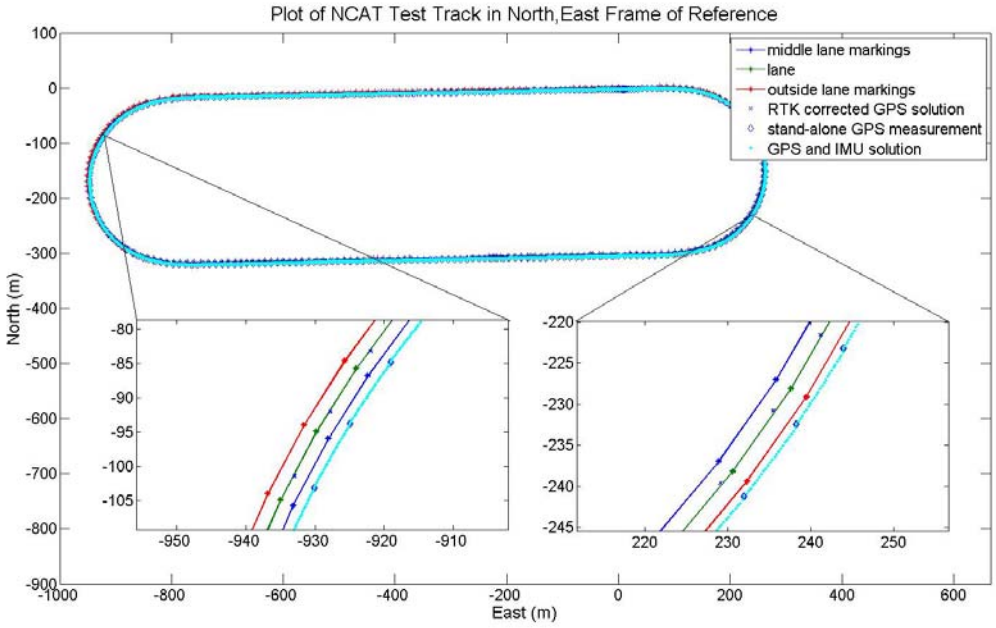

Fig. 8. Plot of GPS, LiDAR, Camera, and IMU Solution with Track Map

The vehicle stops after completing one lap. The vehicle never ventures more than 80 cm from the lane center.

The navigation filter has an output rate that matches the IMU's output rate (50 Hz). The RTK-corrected GPS solution is only available at 2Hz. In order to quantify the navigation filter's error, the RTK-corrected GPS solution is linearly interpolated between GPS measurements. The ECEF coordinates of position is interpolated based on the time between the GPS measurements and desired measurement. These values are then mapped into the road frame to estimate the lateral position in the lane at the desired measurement time.

RESULTS

For validation and comparison reasons, the navigation filter is initially set up to blend the GPS and IMU measurements. Figure 8 shows the trajectory of the x and y states of the navigation filter in the NED coordinate frame. The solution is heavily biased due to the biases in the GPS measurement. Figure 9 shows the lateral position error of the GPS and IMU only navigation filter. The black lines represent the width of a standard lane (12 ft.).

Fig. 9. Lateral Position Error for GPS and IMU only navigation filter

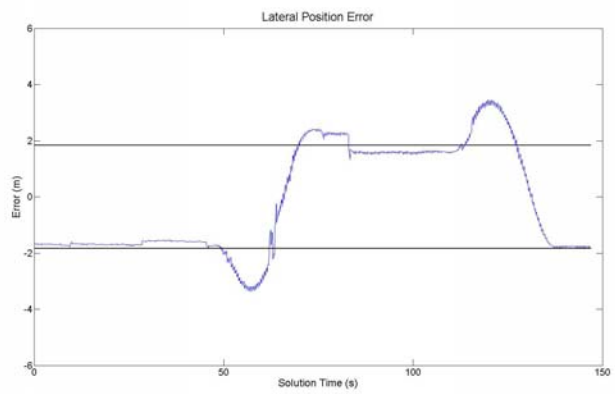

The relatively constant bias in the GPS measurement can be seen in Figure 9. The lateral error remains constant on straightway, and then shifts in the 180° corners. The stand-alone GPS and IMU can not accurately estimate lateral offset in a lane [2]. Vision measurements are perfect to substitute for the lateral position measurement. Vision measurements provide measurements that are much less biased, and vision measurements have a small standard deviation [8].

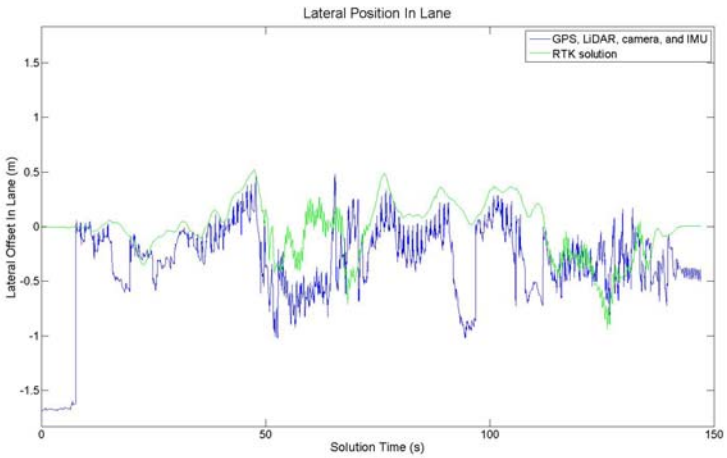

Fig. 10. Plot of GPS, LiDAR, Camera and IMU Lateral Position Estimate Compared to the GPS RTK Solution

Adding vision measurement updates to the navigation filter greatly decreases the lateral position estimate error. Figure 10 shows the lateral position estimate from the GPS, camera, LiDAR, and IMU navigation filter. To give some scale, the y-axis of the plot is spread out 12ft (3.66 m), which is the average width of a highway lane.

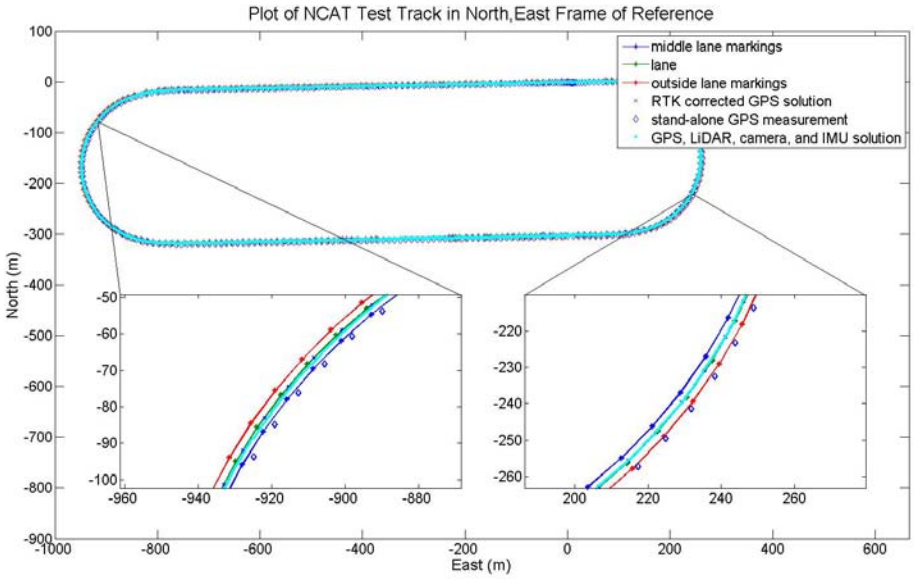

Fig. 11. Plot of GPS, LiDAR, Camera, and IMU Solution with Track Map

The solution never leaves the lane; therefore, the solution is accurate enough track a vehicle's current lane. The solution degrades around 90 seconds due to the large section of missing lane lines on the back straightaway. A few seconds later, the measurement drifts due to the vehicle passing by the off ramp.

The lateral position reported by the interpolated RTK solution is noisy in turns. This is due to the interpolation of the GPS solution, and the interpolation of the curve itself. The interpolation of the curve is introduced when trying to represent the curve in line segments. If the curve is not split into enough road frames, the solution will vary greatly when coordinate frames are changed. If the curve is split into too many road frames, the solution will vary slightly, but at a higher frequency because of the high frequency of coordinate changing. Breaking curves into straight road frames becomes a tradeoff between how much interpolation noise is added and practicality. Too many road frames will result in ambiguity as to what road frame the vehicle currently resides.

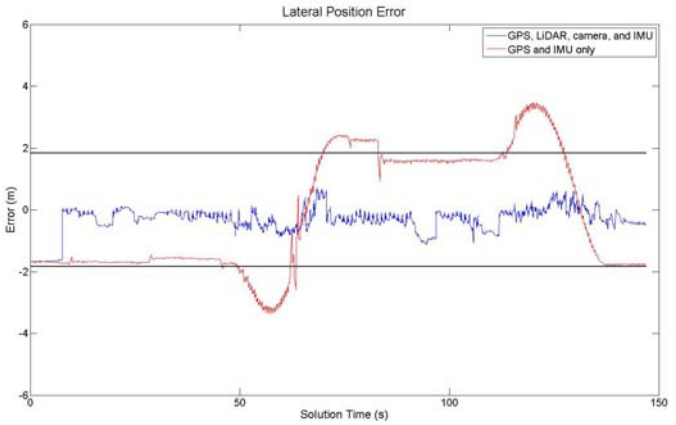

Fig 12. Position Error for the GPS, camera, LiDAR, and IMU Solution

The interpolated RTK solution is used to solve for the error in the navigation filter's lateral estimate. Figure 12 shows a vast improvement in error over the GPS and IMU only solution. The dark lines represent the standard width of a lane.

CONCLUSIONS

The algorithm described will provide an accurate lateral lane position as long as lane markings are available. A more in depth look at time to lane departure is needed to alert the driver before a lane departure [7]. The solution drifts away quickly in areas with poor lane markings. Future work will include examining ways to cut down on estimation drift in the absence of vision measurements. Also, wheel encoders could be used to maintain the observability of the system during GPS outages.

ACKNOWLEDGMENTS

The Federal Highway Administration is funding this project and others across the range of issues that are critical to the transportation industry through the Exploratory Advanced Research (EAR) Program. For more information, see the EAR Web site at http://www.fhwa.dot.gov/advancedresearch/about.cfm#focus"

REFERENCES

[1] J. Britt, "Lane Tracking using Multilayer Laser Scanner to Enhance Vehicle Navigation and Safety Systems," presented at the 2009 International Technical Meeting, Anaheim, California, 2009.

[2] J. Clanton, "GPS and Inertial Sensor Enhancement for Vision-Based Highway Lane Tracking," M.S. thesis, Auburn University, Auburn, Alabama, US, 2006

[3] J. Farell, *Aided Navigation GPS with High Rate Sensors*. New York, New York: McGraw Hill, 2008.

[4] D. Grenjner-Brzezinska and C. Toth, "Performance Study of High-End Dual Frequency GPS Receivers Tightly Integrated with a Strapdown INS," presented at the 2001 Symposium on Mobile Mapping, Cairo, Egypt, Jan. 3-5.

[5] R. E. Kalman, "A New Approach to Linear Filtering and Prediction Problems," *Trans. Of the ASME-Journal of Basic Engineering*, 82 (Series D), pp. 35-45, 1960.

[6] J. Kibbel, Winfried Justus, Kay Fürstenberg, "Lane Estimation and Departure Warning using Multilayer Laserscanner", presented at Proceeding of the 8th International IEEE Conference on Intelligent Transportation Systems, Vienna, Austria, September 13-16, 2005.

[7] S. Mammar, S. Glaser, and M. Netto, "Time to Line Crossing for Lane Departure Avoidance: A Theoretical Study and an Dxperimental Setting," *IEEE Trans. Entelligent Transportation Systems*, vol. 7, pp. 2, June 2006.

[8] C. Rose, "Vehicle Lane Position Estimation with Camera Vision using Bounded Polynomial Interpolated Lines," presented at the 2009 International Technical Meeting, Anaheim, California, 2009.

[9] G. Welch and G. Bishop, "An introduction to the Kalman filter," UNC-Chapel Hill, Chapel Hill, North Carolina, 2006.